

apparent critical Lorentz force and the critical thermal force increases with decreasing film thickness suggests that these current channels are associated with the surface of the specimen. Similar conclusions have been reached from studies of the Nernst effect and the flux flow in thin films of tin and indium.¹⁶ It is interesting to note that the discrepancy between the critical thermal force and the critical Lorentz force disappears in a thick specimen where surface effects can be neglected.²⁷

The present results appear to resolve the controversy between Joiner and Kuhl⁵ and Swartz and Hart⁸ in favor of the surface-current model. In their criticism of the surface flux-pinning model of Swartz and Hart, Joiner and Kuhl argue that apparently the critical current is not a surface current because otherwise the

²⁷ J. Lowell (private communication).

flux-flow resistivity would be reduced and would decrease much more strongly than observed as the magnetic field becomes more aligned with the sample surface. However, since the surface currents affect only the critical-current value and not the flux-flow resistivity, this argument of Joiner and Kuhl seems to be invalid.

ACKNOWLEDGMENTS

The authors are grateful to B. Bryson for his assistance in the sample preparation. A series of useful conversations with H. Berndt, H. Koppe, J. Lowell, and H. A. Ullmaier is gratefully acknowledged. One of us (R. P. H.) would like to express his gratitude to the staff of the Institut Für Festkörper und Neutronenphysik, Kernforschungsanlage Jülich for their kind hospitality.

Intrinsic Fluctuations in Superconducting Rings Containing One-Dimensional Weak Links

D. E. McCUMBER

Bell Telephone Laboratories, Murray Hill, New Jersey 07974

(Received 15 January 1969)

The Langer-Ambegaokar statistical theory of dissipative fluctuations in narrow superconducting channels is extended to describe the quantum transitions of a closed superconducting ring containing a long one-dimensional weak-link section. The external magnetic flux Φ_0 linking the loop is the independent thermodynamic variable. Based upon the Ginzburg-Landau free energy, the theory is expected to accurately describe single-quantum transitions for T near but slightly below T_c . Data reported by Lukens and Goodkind for thin-film Sn rings are reasonably consistent with the theory, but more definitive experimental tests are required.

I. INTRODUCTION

A STATISTICAL model based upon a free-energy function of the Ginzburg-Landau form has been proposed by Langer and Ambegaokar (LA) to describe the onset of dissipation in thin superconducting wires near T_c .¹ Their principal predictions for long, simply connected wires of uniform cross section have been confirmed by Webb and Warburton in experiments on whisker crystals of tin, structures with remarkable uniformity.^{2,3} The original formulas were derived under the assumption that the gauge-invariant phase difference $\Delta\varphi$ across the ends of the wire was held fixed, but they also obtain for long wires under conditions of constant current.⁴ In this paper we develop the corresponding theory of a closed ring of thin superconduct-

ing wire near T_c in a weak quasistatic external magnetic field. The total free energy includes that stored in the wire plus that stored in the field. The analysis is slightly more complicated than the cases considered previously in that the external magnetic field rather than the phase difference $\Delta\varphi$ or the current I is the independent thermodynamic variable.

We do not require that the ring have uniform cross section nor be everywhere thin compared to the coherence length $\xi(T)$, but we do assume that it contains a thin weak-link section of uniform cross-sectional area σ and of length $L \gg \xi(T)$. The weak-link section is "one-dimensional" in the sense that its maximum diameter is everywhere less than $\xi(T)$. Cases with non-uniform cross section or with $L \lesssim \xi(T)$ can be accommodated in the formalism; results for such systems will be described in a later paper. Briefly, the principal effect of variable σ and finite L is to broaden the temperature range of the resistive transition compared to that for a long uniform sample of the same average

¹ J. S. Langer and V. Ambegaokar, *Phys. Rev.* **164**, 498 (1967).

² W. W. Webb and R. J. Warburton, *Phys. Rev. Letters* **20**, 461 (1968).

³ J. Franks, *Acta Met.* **6**, 103 (1958); C. Herring and J. K. Galt, *Phys. Rev.* **85**, 1060 (1952).

⁴ D. E. McCumber, *Phys. Rev.* **172**, 427 (1968).

cross section. Spatial variations in the mean-field critical temperature T_c are an even more serious source of anomalous broadening in thin-film weak links (or microbridges), for example, where it is well known that strain between film and substrate can change T_c by as much as a few tenths of a degree Kelvin.⁵ One important feature of the Webb-Warburton whisker results² is that the range of the resistive transition, although still somewhat larger than predicted by theory for purely intrinsic fluctuations,¹ is an order of magnitude smaller than that previously reported on thin-film samples⁶⁻⁸ and of the order of the fluctuation shift ΔT_c being sought.

Fluctuations in small superconducting loops with point-contact weak links have been studied in a preliminary way at temperatures well below T_c by Zimmerman and Silver.⁹ Experiments which relate more directly to the theory we describe below are those of Lukens and Goodkind on thin-film Sn rings at temperatures near T_c .¹⁰ Their samples were formed by evaporating a 1-mm-wide strip, 1000 Å thick, onto a $\frac{3}{16}$ -in.-diam sapphire tube; each strip was cut to have a weak-link section about 8 μ long with a reduced width of 3 μ. These samples marginally meet the conditions for a one-dimensional uniform-long-wire analysis, but spatial variations in T_c may be a problem as they were previously in simply connected thin-film structures. The experiments do exhibit certain qualitative features predicted by the theory, but there are significant discrepancies which are discussed in Sec. VII.

In Sec. II we briefly describe the statistical model appropriate to the ring geometry. Metastable states in a fixed external magnetic field are described in Sec. III, and the free-energy barriers separating adjacent metastable states in Sec. IV. The master equation governing the time rate of transitions between these states is developed in Sec. V. Two time-scale prefactors are given, one proposed by Lander and Ambegaokar and another derived from the time-dependent Ginzburg-Landau equation. Formulas appropriate to specific experiments are derived in Sec. VI and briefly compared with the Lukens-Goodkind results in Sec. VII.

II. STATISTICAL MODEL

The system with which we are concerned is a superconducting ring of self-inductance L_s in a weak quasi-

⁵ R. D. Parks, in *Fluctuations in Superconductors*, edited by W. S. Goree and F. Chilton (Stanford Research Institute, Menlo Park, Calif., 1968), p. 141.

⁶ R. D. Parks and R. P. Groff, *Phys. Rev. Letters* **18**, 342 (1967).

⁷ T. K. Hunt and J. E. Mercereau, *Phys. Rev. Letters* **18**, 551 (1967).

⁸ R. P. Groff, Š. Marčelja, W. E. Masker, and R. D. Parks, *Phys. Rev. Letters* **19**, 1328 (1967).

⁹ J. E. Zimmerman and A. H. Silver, *Phys. Rev. Letters* **19**, 14 (1967); A. H. Silver and J. E. Zimmerman, *Phys. Rev.* **157**, 317 (1967).

¹⁰ J. E. Lukens and J. M. Goodkind, *Phys. Rev. Letters* **20**, 1363 (1968).

static magnetic field. If I is the current in the ring, the total flux Φ linking the ring is

$$\Phi = \Phi_e - L_s I, \quad (2.1)$$

where Φ_e is the externally applied flux which would link the ring if broken ($I=0$). The total free energy F of a particular state of the system includes that stored in the superconductor plus that stored in the induced field. The infinitesimal change in free energy appropriate to a reversible infinitesimal isothermal change in external flux Φ_e is

$$dF = Id\Phi_e, \quad (2.2a)$$

$$= Id\Phi + L_s IdI, \quad (2.2b)$$

where the second form follows from (2.1) and explicitly exhibits the superconductor and field components.

Following Langer and Ambegaokar,^{1,11} we assume that the free-energy density in the superconductor is a local function at each instant of a complex-valued order parameter $\psi(\mathbf{r})$ which ranges with time in a continuous random fashion over the $\psi(\mathbf{r})$ function space consistent with the required boundary conditions. The free-energy functional $F[\psi(\mathbf{r})]$ formed from the volume integral of this free-energy density and from expressions for the energy stored in the electromagnetic field acts as a mean effective potential driving the order parameter $\psi(\mathbf{r})$. The neighborhood of each point in the order-parameter function space is visited with a frequency proportional to the Boltzmann factor $e^{-F/k_B T}$. Stable and metastable states of the system correspond respectively to absolute and local minima of the functional $F[\psi(\mathbf{r})]$. In a given metastable state, $|\psi(\mathbf{r})|$ will deviate significantly from its average value (at the F minimum) only for points \mathbf{r} near the weak link, so that effectively the free energy F is a functional only of the order parameter $\psi(\mathbf{r})$ in and near the weak link. In narrow links with maximum diameter less than $\xi(T)$, the order parameter is a function only of the dimension along the length of the link, variations of $\psi(\mathbf{r})$ in the transverse directions being suppressed by the Boltzmann factor.

That part of the free energy stored in the superconductor can be written as the sum of two terms, one describing the energy in the weak-link section and a second that in the remainder or "bulk" section of the ring. We approximate the latter by the free energy in equilibrium of a length L_b of wire of uniform cross section σ_b carrying the ring current I . Through terms of order I^2 and to within an additive constant equal to the zero-current condensation energy this is

$$F_b = I^2 \Phi_0^2 l_b / 4\pi\sigma_b H_c^2(T) \xi(T), \quad (2.3)$$

where $l_b \equiv L_b / \xi(T)$ is the length in dimensionless units, $H_c(T)$ is the bulk critical field at temperature T , and

¹¹ J. S. Langer, in *Fluctuations in Superconductors*, edited by W. S. Goree and F. Chilton (Stanford Research Institute, Menlo Park, Calif., 1968), p. 83.

$\Phi_0 = hc/2e$ is the flux quantum.¹² Gaussian units are used throughout.

If we describe the weak-link section by the Ginzburg-Landau formulas,^{1,4} the free-energy functional F for the system is, to within an unimportant additive constant,

$$F(\Phi_e) = \frac{\sigma H_e^2(T)\xi(T)}{4\pi} \int_{-l/2}^{l/2} dx [-f^2(x) + \frac{1}{2}f^4(x) + (df(x)/dx)^2 + (f(x)[d\varphi(x)/dx])^2] + \frac{1}{2}L_e I^2(\Phi_e), \quad (2.4)$$

where $l \equiv L/\xi(T)$ is the length of the weak link in dimensionless units ($l \gg 1$ assumed), where L_e is the effective self-inductance [Eq. (2.3)]

$$L_e = L_e + \Phi_0^2 l_b / 2\pi \sigma_b H_e^2(T)\xi(T), \quad (2.5)$$

and where $f(x)e^{i\varphi(x)}$ is proportional to the gauge-invariant Ginzburg-Landau order parameter in the link.¹² For the weak magnetic fields with which we are here concerned, $\varphi(x)$ differs from the phase of $\psi(\mathbf{r})$ by a line integral of the vector potential.¹³

Whereas $\psi(\mathbf{r})$ is constrained to be strictly periodic (single valued) about the ring, the change $\Delta\varphi$ of the gauge-invariant phase $\varphi(x)$ from one end of the link to the other is a function of the flux Φ through the ring

$$\Delta\varphi = 2\pi\Phi/\Phi_0 - \Delta\varphi_b, \quad \text{modulo } 2\pi \quad (2.6)$$

where $\Phi_0 = hc/2e$ is again the flux quantum and $\Delta\varphi_b$ is the change in gauge-invariant phase across the "bulk" section of the ring

$$\Delta\varphi_b = l_b \Phi_0 I(\Phi_e) / \sigma_b H_e^2(T)\xi(T). \quad (2.7)$$

Combining Eqs. (2.1), (2.6), and (2.7), we find that

$$\Delta\varphi = 2\pi[\Phi_e - L_e I(\Phi_e)]/\Phi_0, \quad \text{modulo } 2\pi \quad (2.8)$$

where L_e is the effective inductance defined in Eq. (2.5). Equations (2.6) and (2.8) are fluxoid quantum conditions.

In the limit $\Delta T \equiv T_c - T \rightarrow 0^+$, the prefactor $\sigma H_e^2(T)\xi(T)/4\pi$ in the first term of (2.4) vanishes as $(\Delta T)^{3/2}$. The second or bulk-correction term in the inductance (2.5) diverges as $(\Delta T_{eb} + \Delta T)^{-3/2}$, where $\Delta T_{eb} \equiv T_{eb} - T_c$ is the difference, if any, between the critical temperature in the bulk section and that in the weak link. The "bulk" properties enter our analysis only through the kinetic inductance $L_e - L_s$.

III. METASTABLE STATES

The metastable states of the system in a fixed external field Φ_e correspond to minima in the free

¹² To minimize the confusion between the lengths (L , L_b) and the inductances (L_s , L_e), we use dimensionless lengths $l = L/\xi(T)$ and $l_b = L_b/\xi(T)$ in our principal equations. These latter should not be confused with carrier mean free paths, which we never consider.

¹³ P.-G. de Gennes, *Superconductivity of Metals and Alloys* (W. A. Benjamin, Inc., New York, 1966), Chap. 7.

energy (2.4) with respect to variations $\{\delta f(x), \delta\varphi(x), \delta I\}$ which satisfy the constraint (2.8) but are otherwise arbitrary.¹⁴ At the extremes of F , the functions $f(x)$ and $\varphi(x)$ satisfy the Ginzburg-Landau equations, which in our notation are

$$d^2 f(x)/dx^2 = -f(x) + f^3(x) + J^2/f^3(x), \quad (3.1a)$$

$$J = f^2(x)[d\varphi(x)/dx], \quad (3.1b)$$

where J is dimensionless, independent of x , and related to the supercurrent I in the sample by

$$I = J\sigma H_e^2(T)\xi(T)/\Phi_0 \equiv lI_0/2\pi, \quad (3.2)$$

where $lI_0/2\pi$ vanishes as $(\Delta T)^{3/2}$ in the limit $\Delta T \rightarrow 0^+$, as is characteristic of the critical current ($J = J_c = 2\sqrt{3}/9$) in the absence of fluctuations. J is constrained by (2.8) to values

$$J_m = 2\pi(\eta - m) / \left[\int_{-l/2}^{l/2} dx f^{-2}(x) + \frac{lL_e I_0}{\Phi_0} \right], \quad (3.3)$$

where m is an integer, and where

$$\eta \equiv \Phi_e/\Phi_0 \quad (3.4)$$

is a convenient measure of the external flux in units of the flux quantum. Only values of m such that $|J_m| < J_c$ are admissible.

It is useful to express J_m , $0 \leq |J_m| < J_c$, in terms of a parameter κ_m such that

$$J_m = \kappa_m(1 - \kappa_m^2), \quad \kappa_m^2 < \frac{1}{3}. \quad (3.5)$$

That solution of Eqs. (3.1)–(3.3) which corresponds to a local free-energy minimum has

$$f^2(x) = 1 - \kappa_m^2, \quad (3.6a)$$

$$\varphi(x) = \kappa_m x + \varphi_0, \quad \Delta\varphi = l\kappa_m, \quad (3.6b)$$

where from (3.3)

$$\kappa_m = 2\pi(\eta - m)/l[1 + (1 - \kappa_m^2)L_e I_0/\Phi_0]. \quad (3.7)$$

The corresponding ring current and free energy are

$$I_m(\Phi_e) = (\eta - m)(1 - \kappa_m^2)I_0/[1 + (1 - \kappa_m^2)L_e I_0/\Phi_0] \quad (3.8)$$

and

$$F_m(\Phi_e) = -l^2\Phi_0 I_0(1 - \kappa_m^2)^2 \times (1 - 2L_e I_0 \kappa_m^2/\Phi_0)/16\pi^2, \quad (3.9)$$

respectively. The free energy is an absolute minimum in that state for which the circulating current magnitude $|I_m|$ is a minimum ($m = \text{integer nearest } \eta$).

The integer m is a fluxoid quantum number. It is constrained by the requirement that Eqs. (3.6)–(3.9) describe a local free-energy minimum to values such that $|J_m| < J_c$ or, equivalently, $\kappa_m^2 < \frac{1}{3}$. Neglecting boundary effects at the end of a short wire ($l \lesssim 1$), we can usefully

¹⁴ We implicitly only consider the case $l \gg 1$, for which one has the additional boundary condition $\delta f/df/dx = 0$ at $x = \pm \frac{1}{2}l$.

distinguish three qualitatively different cases:

$$l(1+2L_e I_0/3\Phi_0) \leq \pi\sqrt{3} \quad (3.10a)$$

$$> \pi\sqrt{3} \quad (3.10b)$$

$$\gg \pi\sqrt{3}. \quad (3.10c)$$

The last two cases differ by the degree of inequality. In the first case there is at most one admissible quantum number and sometimes none. A particular integer m is admissible with $\kappa_m^2 < \frac{1}{3}$, when the external field $\Phi_e = \eta\Phi_0$ is such that

$$|\eta - m| < l(1+2L_e I_0/3\Phi_0)2\pi\sqrt{3}. \quad (3.11)$$

When (3.10a) obtains ranges of external field exist (η approximately half integral) for which (3.11) cannot be satisfied for any integer m . For such fields the weak link becomes normal. Examples for point-contact weak links are reported by Zimmerman and Silver.⁹ When (3.10b) obtains, there is always at least one and possibly several admissible quantum numbers. By adjusting the temperature T near T_c , one can vary the parameters on the right-hand side of (3.11) and measure a critical temperature $T_c(\eta)$ for which the system will just remain superconducting for some m at a field $\eta = \Phi_e/\Phi_0$; in essence, this is the experiment of Little and Parks.^{15,16}

In what follows, we are only concerned with $l \gg 1$ and the case (3.10c). Many quantum numbers m are admissible for each value of the field parameter η , and adjacent values of κ_m are sufficiently closely spaced that to the required accuracy

$$\kappa_{m+1} - \kappa_m = -2\pi/l \{1 + [1 - 3\kappa_m^2]L_e I_0/\Phi_0\}, \quad (3.12a)$$

$$I_{m+1} - I_m = -[1 - 3\kappa_m^2]I_0 / \{1 + [1 - 3\kappa_m^2]L_e I_0/\Phi_0\}, \quad (3.12b)$$

and

$$F_{m+1} - F_m = -\frac{1}{2}\Phi_0(I_{m+1} + I_m), \quad (3.12c)$$

where $m = m$, $m+1$, or an intermediate value.

Under conditions for which the Langer-Ambegaokar model is valid, the long-link condition $l \gg 1$ implies that the total condensation free energy of the weak link

$$|F_n - F_s|_{\text{weak link}} = l\sigma H_e^2(T)\xi(T)/8\pi = l^2\Phi_0 I_0/16\pi^2 \quad (3.13)$$

is very much greater than the thermal energy $k_B T$. Only those states for which $\kappa_m^2 \ll \frac{1}{3}$ will contribute significantly to the system statistics. For such states Eq. (3.9) simplifies to

$$F_m(\Phi_e) = -l^2\Phi_0 I_0/16\pi^2 + \beta k_B T(\eta - m)^2, \quad (3.14)$$

where

$$\beta = \Phi_0 I_0/2k_B T(1 + L_e I_0/\Phi_0) \geq 0. \quad (3.15)$$

States for which the whole link is normal or for which $\kappa_m^2 \approx \frac{1}{3}$ will be suppressed by the Boltzmann factor.

¹⁵ W. A. Little and R. D. Parks, Phys. Rev. Letters **9**, 9 (1962); R. D. Parks and W. A. Little, Phys. Rev. **133**, A97 (1964).

¹⁶ R. P. Groff and R. D. Parks, Phys. Rev. **176**, 567 (1968).

The difference $|I_{m+1} - I_m|$ in (3.12b) is less than the lesser of $(1 - 3\kappa_m^2)I_0$ and Φ_0/L_e , where the latter bound obtains in the limit $L_e I_0/\Phi_0 \gg 1/(1 - 3\kappa_m^2) \approx 1$. As $\Delta T = T_c - T$ increases from zero, $|I_{m+1} - I_m|$ increases with I_0 proportionally to ΔT until finally, when $I_0 \gg \Phi_0/L_e$, it saturates at the value Φ_0/L_e . For ΔT large, L_e approximates L_s and the flux Φ linking the ring [Eq. (2.1)] is quantized in units of the flux quantum.¹⁷

IV. FREE-ENERGY BARRIERS

With Φ_e fixed, the system will gradually relax to quantum states for which the circulating current I is small. The steady-state probability that the system has a particular fluxoid quantum number m is approximately proportional to the Boltzmann factor $\exp[-F_m(\Phi_e)/k_B T]$.¹⁸ We wish to determine the probability per unit time that the system will relax from a highly excited state (I large) to a less excited state and the probability per unit time that the system will transfer from one state with appreciably steady-state probability to another. These rates, which we discuss in detail in Secs. V and VI, are sensitive to the height of the free-energy barrier between adjacent minima in the ψ function space.¹ The minimum barrier corresponds to motion over a saddle point of $F(\psi)$. These saddle points are extrema of F and satisfy the Ginzburg-Landau equation (3.1) and the constraint equation (2.8) [or (3.3) suitably interpreted]. The nature of the saddle-point solutions of Eq. (3.1) has been described in detail by Langer and Ambegaokar.¹

The saddle-point barrier between the m and $m+1$ minima described in Sec. III is conveniently characterized by current parameters $\bar{\kappa}_m$, \bar{J}_m , and \bar{I}_m and by the saddle-point free energy \bar{F}_m . The current parameters are related through Eqs. (3.2) and (3.5). In the large- l limit with which we are here concerned, the function $f(x)$ at the saddle is such that^{4,19}

$$\bar{J}_m \int_{-\frac{1}{2}l}^{\frac{1}{2}l} dx f^{-2}(x) = l\bar{\kappa}_m + 2 \tan^{-1} \left(\frac{1 - 3\bar{\kappa}_m^2}{2\bar{\kappa}_m^2} \right)^{1/2} \quad (4.1)$$

and

$$\bar{F}_m = -l^2\Phi_0 I_0 [(1 - \bar{\kappa}_m^2)^2 (1 - 2L_e I_0 \bar{\kappa}_m^2/\Phi_0) - 8\sqrt{2}(1 - 3\bar{\kappa}_m^2)^{1/2}/3l]/16\pi^2. \quad (4.2)$$

¹⁷ B. S. Deaver and W. M. Fairbank, Phys. Rev. Letters **7**, 43 (1961); R. Doll and M. Nábauer, *ibid.* **7**, 50 (1961).

¹⁸ More precisely, the probability is proportional to the Boltzmann factor times the volume of ψ -function space for which $F(\psi)$ is within a $k_B T$ neighborhood of the free-energy minimum F_m . This volume depends upon the curvature of $F(\psi)$ at $F = F_m$ in ψ -function space and varies slowly with the index m . It enters a thermodynamic description through the entropy associated with order-parameter fluctuations about the metastable-state solutions $\psi_m(\mathbf{r})$ [Eq. (5.4)]. To the extent that this entropy varies with m , F is an energy rather than a true free energy (Ref. 25).

¹⁹ Here $\tan^{-1}(\dots)$ is the principal value of the arctangent. Its sign and that of $[(1 - 3\bar{\kappa}_m^2)/2\bar{\kappa}_m^2]^{1/2}$ is the same as that of $\bar{\kappa}_m$.

The parameter $\bar{\kappa}_m$ lies between κ_m and κ_{m+1} and closer to the larger in magnitude. This fact fixes the integer index in (3.3) and together with (4.1) gives [cf. (3.7)]

$$\bar{\kappa}_m = \frac{2\pi\{\eta - m - \pi^{-1} \tan^{-1}[(1 - 3\bar{\kappa}_m^2)/2\bar{\kappa}_m^2]^{1/2}\}}{l[1 + (1 - \bar{\kappa}_m^2)L_e I_0/\Phi_0]}, \quad (4.3a)$$

for $\bar{\kappa}_m > 0$ and

$$\bar{\kappa}_m = \frac{2\pi\{\eta - m - 1 - \pi^{-1} \tan^{-1}[(1 - 3\bar{\kappa}_m^2)/2\bar{\kappa}_m^2]^{1/2}\}}{l[1 + (1 - \bar{\kappa}_m^2)L_e I_0/\Phi_0]}, \quad (4.3b)$$

for $\bar{\kappa}_m < 0$. The case $\bar{\kappa}_m = 0$ follows as a limiting case. To avoid excessive duplication, we limit ourselves below to the case $\kappa_m \geq \bar{\kappa}_m > 0$; the case $\bar{\kappa}_m < 0$ is easily treated by symmetry arguments or by the use of (4.3b).

It is useful to consider separately the two cases $\bar{\kappa}_m > 0 \gtrsim \kappa_{m+1}$ and $\kappa_{m+1} > 0$. In the first case ($\bar{\kappa}_m > 0 \gtrsim \kappa_{m+1}$) we have under the same conditions for which Eqs. (3.12) apply

$$\bar{\kappa}_m - \kappa_m = -\pi/l[1 + L_e I_0/\Phi_0], \quad (4.4a)$$

$$\bar{I}_m - I_m = -\frac{1}{2}I_0/[1 + L_e I_0/\Phi_0], \quad (4.4b)$$

and²⁰

$$\Delta F_m^+ \equiv \bar{F}_m - F_m = l\Phi_0 I_0 \sqrt{2}/6\pi^2 - \frac{1}{4}\Phi_0(\bar{I}_m + I_m), \quad (4.5a)$$

$$\Delta F_m^- \equiv \bar{F}_{m-1} - F_m = \Delta F_m^+ + \Phi_0 I_m, \quad (4.5b)$$

where the ΔF_m^\pm are free-energy barriers appropriate to transitions from the metastable state m to the adjacent states $m \pm 1$, respectively. As one would expect from symmetry, these two barriers are equal if $I_m = 0$. If $I_m > 0$ ($\kappa_m > 0$), the condition $\Delta F_m^- > \Delta F_m^+$ is consistent with our assertion that relaxation is toward states with minimum circulating current.

When $\kappa_{m+1} > 0$, we find from Eqs. (3.12) and (4.1)-(4.3) that

$$\bar{\kappa}_m - \kappa_m = -2 \tan^{-1}[(1 - 3\kappa_m^2)/2\kappa_m^2]^{1/2} / l[1 + (1 - 3\kappa_m^2)L_e I_0/\Phi_0], \quad (4.6a)$$

$$\bar{I}_m - I_m = -(1 - 3\kappa_m^2)I_0 \tan^{-1}[(1 - 3\kappa_m^2)/2\kappa_m^2]^{1/2} / \pi[1 + (1 - 3\kappa_m^2)L_e I_0/\Phi_0], \quad (4.6b)$$

and

$$\Delta F_m^+ = l\Phi_0 I_0 \sqrt{2}(1 - 3\kappa_m^2)^{1/2}/6\pi^2 - [\Phi_0(\bar{I}_m + I_m)/2\pi] \times \tan^{-1}[(1 - 3\kappa_m^2)/2\kappa_m^2]^{1/2}, \quad (4.7a)$$

$$\Delta F_m^- = \Delta F_m^+ + \Phi_0 I_m, \quad \bar{m} = m - \frac{1}{2} + (1/\pi) \times \tan^{-1}[(1 - 3\kappa_m^2)/2\kappa_m^2]^{1/2}. \quad (4.7b)$$

Relaxation again proceeds toward states with minimum circulating current. In the limit $\kappa_m \rightarrow 1/\sqrt{3}$ for which the current I_m approaches the limiting critical current

²⁰ From the definition (3.2), I_0 varies as l^{-1} , so that lI_0 is independent of the length l .

$I_c = lI_0\sqrt{3}/9\pi$, ΔF_m^+ vanishes as

$$(1 - 3\kappa_m^2)^{5/2}\Phi_0 I_c 3(\sqrt{6})/20$$

but ΔF_m^- remains finite at $\Phi_0 I_c$.

V. TRANSITIONS BETWEEN METASTABLE STATES

In the Langer-Ambegaokar model the free-energy barriers ΔF_m^\pm dominate the rates of transitions between metastable states. If $P_m(t)$ is the probability that the system is in metastable state m (Sec. III) at time t , they postulate that the system is always in at least one such state,

$$\sum_m P_m(t) = 1, \quad P_m(t) \geq 0 \quad (5.1)$$

and that

$$\partial P_m(t)/\partial t = \{P_{m-1}(t)\Omega_{m-1}^+(T)e^{-\Delta F_{m-1}^+/k_B T} + P_{m+1}(t)\Omega_{m+1}^-(T)e^{-\Delta F_{m+1}^-/k_B T} - P_m(t)[\Omega_m^+(T)e^{-\Delta F_m^+/k_B T} + \Omega_m^-(T)e^{-\Delta F_m^-/k_B T}]\}, \quad (5.2)$$

where $\Omega_m^\pm(T)$ are rate parameters which depend only weakly on the index m and the temperature T , $0 < T \leq T_c$. If $S_m(T)$ is the entropy associated with order-parameter fluctuations in the neighborhood of the metastable state of Eqs. (3.6)-(3.9) and if $\bar{S}_m(T)$ is the corresponding entropy for the saddle point of Eqs. (4.1)-(4.3), the $\Omega_m^\pm(T)$ have the form^{21,22}

$$\Omega_m^+(T) = R e^{-(\bar{S}_m - S_m)/k_B}, \quad (5.3a)$$

$$\Omega_m^-(T) = R e^{-(\bar{S}_{m-1} - S_m)/k_B}, \quad (5.3b)$$

where R is a time-scale prefactor. Equations (5.2) and (5.3) have the equilibrium solution¹⁸

$$P_m = \exp\frac{-(F_m - TS_m)}{k_B T} / \sum_n \exp\frac{-(F_n - TS_n)}{k_B T}, \quad (5.4)$$

which predicts state- m occupation proportional to the Boltzmann factor $\exp[-(F_m - TS_m)/k_B T]$. In a thermodynamic picture, the combination $(F_m - TS_m)$ is the total Helmholtz free energy of the system in state m .¹⁸

Since the free-energy barriers ΔF_m^\pm enter Eq. (5.2) exponentially, but the $\Omega_m^\pm(T)$ enter only linearly, predictions based upon (5.2) are expected to be relatively insensitive (logarithmic) to errors in $\Omega_m^\pm(T)$. Langer and Ambegaokar speculate within this latitude that $\Omega_m^\pm(T) = \Omega(T)$ with¹

$$\Omega(T) = l\sigma\xi(T)n_e/\tau, \quad (5.5)$$

where $\tau \sim 10^{-12}$ sec is a typical electron-scattering time in the normal state and $l\sigma\xi(T)n_e$ equals the number of conduction electrons in the volume $l\sigma\xi(T)$ of the weak link.¹² This choice is consistent with the experimental

²¹ R. Landauer and J. A. Swanson, Phys. Rev. **121**, 1668 (1961).

²² J. S. Langer, Phys. Rev. Letters **21**, 973 (1968).

observations of Webb and Warburton,² but it gives a transition rate which is much greater than that reported by Lukens and Goodkind.¹⁰

The time-dependent Ginzburg-Landau equation derived by Schmid²³ and others²⁴ leads to rate parameters different from (5.5). In the time-dependent theory, small fluctuations of the normalized order parameter decay to a minimum- F configuration according to the equation

$$\tau(T)[(\partial/\partial t) - i(2e/\hbar)V]\psi = (1 - |\psi|^2)\psi + [(\partial/\partial x) + i\xi(T)(2e/\hbar c)A_x]^2\psi, \quad (5.6)$$

where x is measured in units of the coherence length $\xi(T)$, $V(x,t)$ is the electrochemical potential, $\mathbf{A}(x,t)$ is the vector potential, and

$$\tau(T) = \pi\hbar/8k_B\Delta T. \quad (5.7)$$

In steady state, Eq. (5.6) reduces to the familiar Ginzburg-Landau Eq. (3.1). If Eq. (5.6) describes the time development of the order parameter $\psi(x)$ near the free-energy saddle points as well as near the minima, it follows for a long thin wire link with $\kappa_m^2 \ll \frac{1}{3}$ that $\Omega_m^\pm(T) = \Omega(T)$, where to within a factor of order unity^{21,22,25}

$$\Omega(T) = [3^{1/2}l/2\pi^{3/2}\tau(T)][\Delta F(T)/k_B T]^{1/2}, \quad (5.8)$$

with

$$\Delta F(T) = \sigma H_c^2(T)\xi(T)\sqrt{2}/3\pi = l\Phi_0 J_0 \sqrt{2}/6\pi^2, \quad (5.9)$$

the free-energy barrier (4.5) appropriate to $\kappa_m^2 = 0$. Equation (5.8) and indeed the basic Langer-Ambegaokar thermal-activation model is only valid for $(T_c - T)$ sufficiently positive that

$$[\Delta F(T)/k_B T]^{1/2} \exp[-\Delta F(T)/k_B T] \ll 1, \quad (5.10)$$

which is generally not a very severe restriction. In the limit $\Delta T \rightarrow 0$, $\Omega(T)$ in (5.8) vanishes as $(\Delta T)^{9/4}$.

Equation (5.8) differs from (5.5) in its functional dependence on temperature, on electron mean free path (in both the dirty and clean limits), and on wire cross-sectional area σ . For the one-dimensional wire both expressions are proportional to the length l .

The available experimental evidence is inconclusive, although the prefactors (5.8) are approximately ten orders of magnitude less than those of (5.5) for both the Webb-Warburton and Lukens-Goodkind experiments.^{2,10} The different temperature, mean-free-path, and cross-section dependence of (5.5) and (5.8) is not noticeable over the ranges studied but the magnitude difference is. The Webb-Warburton measurements of critical current versus ΔT fit the Langer-Ambegaokar estimate (5.5) very well but give a zero-current temperature shift ΔT_c approximately twice that predicted from (5.8). There is some evidence that internal strains

increase the observed temperature shift even in the nearly ideal whisker crystals,²⁶ but it would be surprising if the Webb-Warburton data on different samples were so uniformly displaced.²⁷

Whereas Webb and Warburton measured the onset of dissipative fluctuations by detecting a small finite voltage (~ 2 nV = 10^6 transitions/sec), Lukens and Goodkind measured the rate $\Gamma(T)$ directly [for $\Gamma(T) = 0.1$ - 10 sec⁻¹] by monitoring the flux Φ through a loop of the type we have been considering. (Formulas specific to their experiments are derived and discussed in Secs. VI and VII.) Their published results¹⁰ favor Eq. (5.8), but other recent data are more consistent with (5.5).²⁸ A precise theoretical interpretation is complicated by the geometric and compositional uncertainties of the thin-film circuit.

VI. BEHAVIOR IN SIMPLE EXPERIMENTS

In what follows, we use the results derived above to analyze a sequence of conceptually simple experiments. The experiments we consider are basically those of Lukens and Goodkind¹⁰; their data are briefly discussed in Sec. VII.

Given the geometry described in Secs. I and II, we assume that the external flux $\Phi_e(t) = \eta(t)\Phi_0$ is a known controlled variable and that either the total flux $\Phi(t)$ linking the loop or the loop current $I(t)$ is accessible for measurement. The flux $\Phi(t)$ and the current $I(t)$ are related through Eq. (2.1). Because the Langer-Ambegaokar analysis we have outlined is only valid under conditions for which states with $\kappa_m^2 \ll \frac{1}{3}$ dominate (Sec. III), we can assume $\Omega_m^\pm(T) = \Omega(T)$ in (5.2) and neglect the index m in the entropy $S_m(T) = S(T)$ in (5.3).

A. Equilibrium Expectation Values

If the external-field parameter $\eta(t)$ is swept sufficiently slowly (Sec. VI C), the system remains close to equilibrium, and the different quantum states are occupied with a probability

$$P_m(t) = P[\eta(t) - m]^0, \quad (6.1)$$

where from (3.14) and (5.4)

$$P(z)^0 = \exp(-\beta z^2) / \sum_n \exp[-\beta(z-n)^2]. \quad (6.2)$$

The function $P(z)^0$ has been plotted for different values of β in Fig. 1.

The average circulating current in the ring when

²⁶ J. H. Davis, M. J. Skove, and E. P. Stillwell, *Solid State Commun.* **4**, 597 (1966).

²⁷ W. W. Webb, in *Fluctuations in Superconductors*, edited by W. S. Goree and F. Chilton (Stanford Research Institute, Menlo Park, Calif., 1968), p. 159.

²⁸ J. E. Lukens and J. M. Goodkind (private communication).

²³ A. Schmid, *Physik Kondensierten Materie* **5**, 302 (1966).

²⁴ E. Abrahams and T. Tsuneto, *Phys. Rev.* **152**, 416 (1966); E. Abrahams and J. W. F. Woo, *Phys. Letters* **27A**, 117 (1968).

²⁵ D. E. McCumber and B. I. Halperin (to be published).

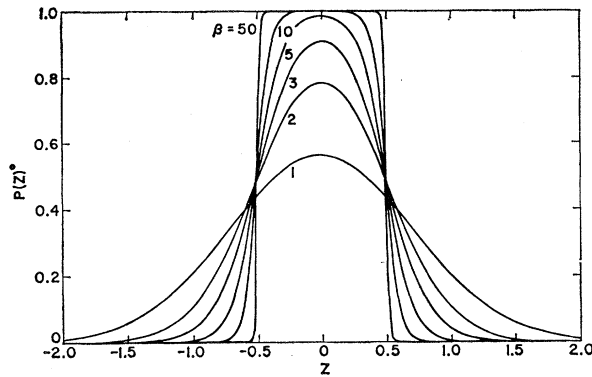


FIG. 1. Equilibrium distribution function $P(z)^0$ of Eq. (6.2) for different values of β . In the limit $\beta \ll 1$, $P(z)^0 = (\beta/\pi)^{1/2} \exp(-\beta z^2)$; in the limit $\beta \gg 1$, $P(z)^0 = 1$ for $|z| < \frac{1}{2}$ and zero for $|z| > \frac{1}{2}$.

(6.1) obtains is $(\kappa_m^2 \ll \frac{1}{3})$

$$\langle I(t) \rangle_{\eta\beta} = \sum_m I_m P[\eta(t) - m]^0 \quad (6.3a)$$

$$= 2\beta \langle \eta(t) - m \rangle_{\eta\beta} I_T, \quad (6.3b)$$

where

$$I_T = k_B T / \Phi_0 = 6.676 \times 10^{-9} T (\text{°K}) A \quad (6.4)$$

and

$$\langle \eta - m \rangle_{\eta\beta} = \sum_m (\eta - m) \times \exp[-\beta(\eta - m)^2] / \sum_n \exp[-\beta(\eta - n)^2]. \quad (6.5)$$

The average $\langle \eta - m \rangle_{\eta\beta}$ has been plotted as a function of η for different β in Fig. 2. It is always periodic in the field parameter η and has a magnitude bounded by the $\beta \rightarrow \infty$ result

$$\langle \eta - m \rangle_{\eta\infty} = \eta(t) - [\text{integer nearest } \eta(t)]. \quad (6.6)$$

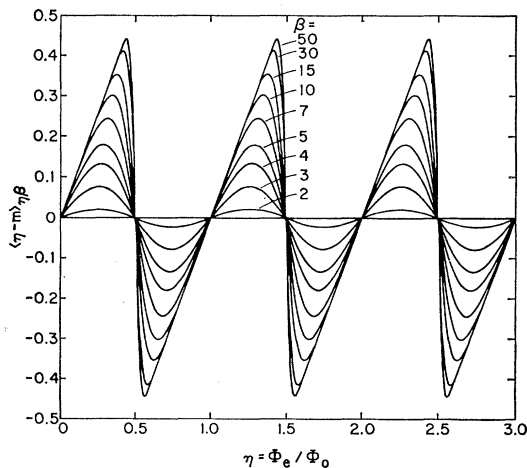


FIG. 2. Ensemble average $\langle \eta - m \rangle_{\eta\beta}$ of Eq. (6.5) as a function of η for different values of β .

For $\beta \lesssim 1$, Eq. (6.5) asymptotically approximates

$$\langle \eta - m \rangle_{\eta\beta} = (2\pi/\beta) e^{-\pi^2/\beta} \sin 2\pi\eta, \quad (6.7)$$

which vanishes very rapidly as β decreases.

The result (6.3) is very important. The periodicity in η permits calibration of a flux- $\Phi_e(t)$ source and of a flux- $\Phi(t)$ detector in units of the flux quantum Φ_0 . The important parameter β can be determined from the maximum excursion with η of the ratio $\langle I(t) \rangle_{\eta\beta} / I_T$. The theoretical excursion $2\beta[\langle \eta - m \rangle_{\max} - \langle \eta - m \rangle_{\min}]$ as determined from curves like those in Fig. 2 is plotted as a function of β in Fig. 3(a).

If the superconductor in the "bulk" section of the ring is identical to that in the weak link ($\Delta T_{eb} = 0$), it

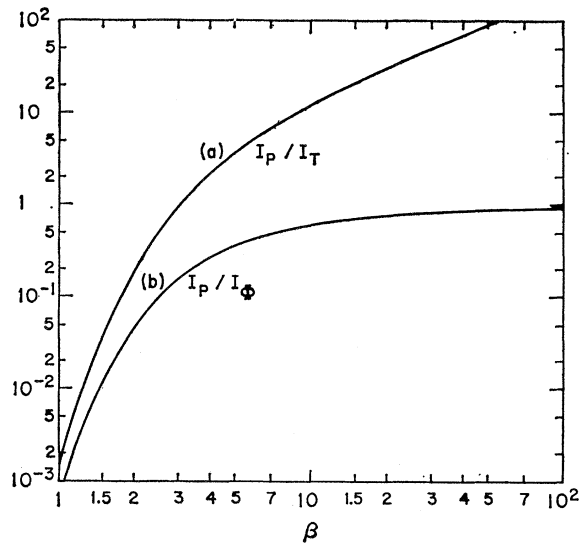


FIG. 3. Maximum excursion $I_p(\beta)$ with external field η of the ensemble-averaged current $\langle I(t) \rangle_{\eta\beta}$ as a function of β . (a) $I_p / I_T = 2\beta[\langle \eta - m \rangle_{\max} - \langle \eta - m \rangle_{\min}]$ with $I_T = k_B T / \Phi_0$; (b) $I_p / I_\Phi = [\langle \eta - m \rangle_{\max} - \langle \eta - m \rangle_{\min}]$ with $I_\Phi = \Phi_0 / L_s$. The results of part (b) are only valid in the limit that β has its saturation value $\beta_\infty = \Phi_0^2 / 2L_s k_B T$. The extrema $\langle \eta - m \rangle_{\max/\min}$ are determined from curves like those in Fig. 2.

follows from (2.5), (3.2), and (3.15) that¹²

$$\beta = \frac{\Phi_0 I_0 / 2k_B T}{(1 + l_b \sigma / l \sigma_b) + L_s I_0 / \Phi_0}. \quad (6.8)$$

For $\Delta T = T_c - T \ll T_c$, $I_0(T)$ is proportional to ΔT and

$$\beta = \beta_\infty \Delta T / (\Delta T + \Delta T_\beta), \quad (6.9a)$$

where

$$\beta_\infty = \Phi_0^2 / 2L_s k_B T, \quad (6.9b)$$

and

$$\frac{1}{\Delta T_\beta} = \frac{L_s}{\Phi_0(1 + l_b \sigma / l \sigma_b)} \frac{dI_0}{dT}. \quad (6.9c)$$

As ΔT increases from zero, the parameter β_∞ increases linearly with ΔT until it saturates at a value β_∞ in-

versely proportional to L_s . From Eqs. (6.3b), (6.4), and (6.9b), it follows in this *saturated* case that

$$\langle I(t) \rangle_{\eta\beta} = \langle \eta - m \rangle_{\eta\beta} I_\Phi, \quad (6.3')$$

where $I_\Phi \equiv \Phi_0/L_s$. The maximum excursion with η of the ratio $\langle I(t) \rangle_{\eta\beta}/I_\Phi$ as given by (6.3') is plotted as a function of $\beta = \beta_\infty$ in Fig. 3(b).

B. Transitions near Equilibrium

Experiments testing the expressions of Sec. VI A do not really test the fluctuation dynamics of the Langer-Ambegaokar theory but rather the probabilities (6.1). Useful information about fluctuation dynamics can be obtained by observing the rate at which a system near equilibrium randomly jumps from one energetically accessible quantum state to another.

The simplest case is that for which the external flux Φ_e is fixed at a half-integral multiple of the flux quantum Φ_0 , and ΔT is large enough that $\beta \geq 2$. Only the two lowest-free-energy quantum states ($m=0$ and 1, say) will be significantly occupied, and they will be occupied with equal *a priori* probability. Equations (5.1) and (5.2) reduce in this case to

$$1 = P_0(t) + P_1(t), \quad (6.10a)$$

$$\partial P_1(t)/\partial t = -\Gamma(T)[P_1(t) - P_0(t)], \quad (6.10b)$$

where the transition rate

$$\Gamma(T) = \Omega(T) \exp\left(-\frac{l\Phi_0 I_0 \sqrt{2}}{6\pi^2 k_B T} - \frac{1}{4}\beta\right). \quad (6.11)$$

The dominant temperature dependence is generally that of $lI_0 \propto (\Delta T)^{3/2}$ in the exponent.

If $\beta < 2$, it is necessary to consider additional quantum states. The analysis is mathematically tedious but straightforward. For example, if the four lowest-energy states are important ($m = -1$ to 2, say), Eqs. (6.10) become

$$1 = P_{-1}(t) + P_0(t) + P_1(t) + P_2(t), \quad (6.12a)$$

$$\partial P_2/\partial t = \Gamma(T)[e^{-\beta}P_1(t) - e^\beta P_2(t)], \quad (6.12b)$$

$$\partial P_1/\partial t = \Gamma(T)[e^\beta P_2(t) - (1 + e^{-\beta})P_1(t) + P_0(t)], \quad (6.12c)$$

$$\partial P_0/\partial t = \Gamma(T)[P_1(t) - (1 + e^{-\beta})P_0(t) + e^\beta P_{-1}(t)]. \quad (6.12d)$$

With β known from measurements of the type described in Sec. VI A, the experiments again determine $\Gamma(T)$.

If $\eta = \Phi_e/\Phi_0$ is not precisely half integral, the rate for increasing quantum number m will be different from the rate for m decreasing. However, the average period for a fluctuation cycle—that is, for fluctuations to return m back to its initial value—is unchanged to first order in the field deviation $\Delta\eta$. More precisely, the average period in the two-state system of Eqs. (6.10) is increased by the factor $\cosh\beta\Delta\eta$.

C. Transitions Farther from Equilibrium

If the field parameter $\eta(t)$ increases at a slow uniform rate η' , the system remains close to equilibrium and

Eqs. (6.1)–(6.9) apply. The circulating current oscillates periodically about a zero time-averaged value. For larger rates η' , the quantum index m increases in steady state at the same average rate as $\eta(t)$ but lags behind the equilibrium average value $\langle m \rangle_{\eta\beta}$ predicted from Eq. (6.5). The circulating current oscillates periodically about a nonzero time-averaged value $I_a(\eta')$. Measurement of $I_a(\eta')$ provides a test of the dynamic theory farther from equilibrium than in the experiments of Sec. VI B.

In steady state with $\eta' = d\eta/dt$ constant, the probabilities $P_m(t)$ are functions of the difference $[\eta(t) - m]$,

$$P_m(t) = P[\eta(t) - m], \quad (6.13)$$

where $P(z) = P(z)^0$ in the limit $\eta' \rightarrow 0$ (Sec. VI A). Assuming as before that $\kappa_m^2 \ll \frac{1}{3}$ and $\Omega_m^\pm(T) = \Omega(T)$, we find from Eqs. (4.7), (5.2), and (6.13) that

$$\eta' [dP(z)/dz] = \Gamma(T) [e^{\beta(z+1)}P(z+1) + e^{-\beta(z-1)}P(z-1) - (e^{\beta z} + e^{-\beta z})P(z)], \quad (6.14)$$

where $\Gamma(T)$ is defined in (6.11). The boundary conditions are $P(z) \rightarrow 0$ for $|z| \rightarrow \infty$ and, from (5.1),

$$\sum_m P(z-m) = 1, \quad P(z) \geq 0 \quad (6.15)$$

for all real z . The first of Eqs. (6.15) implies

$$\int_{-\infty}^{\infty} dz P(z) = 1, \quad (6.16)$$

but not conversely.

The first or z moment of (6.14) gives, with (6.16),

$$\eta' = 2\Gamma(T) \int_{-\infty}^{\infty} dz P(z) \sinh\beta z; \quad (6.17a)$$

the $\cosh m\beta z$ moment gives

$$\begin{aligned} (m\beta\eta'/\Gamma) \int_{-\infty}^{\infty} dz P(z) \sinh m\beta z \\ = (1 - e^{-m\beta}) \int_{-\infty}^{\infty} dz P(z) \cosh[(m+1)\beta z] - (e^{m\beta} - 1) \\ \times \int_{-\infty}^{\infty} dz P(z) \cosh[(m-1)\beta z]; \end{aligned} \quad (6.17b)$$

and the $\sinh m\beta z$ moment gives

$$\begin{aligned} (m\beta\eta'/\Gamma) \int_{-\infty}^{\infty} dz P(z) \cosh m\beta z \\ = (1 - e^{-m\beta}) \int_{-\infty}^{\infty} dz P(z) \sinh[(m+1)\beta z] - (e^{m\beta} - 1) \\ \times \int_{-\infty}^{\infty} dz P(z) \sinh[(m-1)\beta z]. \end{aligned} \quad (6.17c)$$

The time-averaged value of $\langle \eta(t) - m \rangle_{\eta\beta}$ is ($\eta' \geq 0$)

$$\bar{z} = \int_{-\infty}^{\infty} dz z P(z) \leq \eta' / 2\Gamma\beta, \quad (6.18)$$

where the second equality obtains only if $|\beta z| \ll 1$ for all important z . The time-averaged current is

$$I_a(\eta') = 2\beta\bar{z}I_T, \quad (6.19)$$

where I_T is defined in (6.3b). For the special case $\eta' = 0$, these expressions are consistent with the solution $P(z) = P(z)^0$ of Eq. (6.2).

It is obvious from the complexity of the "simple" $\eta' = 0$ solution (6.2) that Eq. (6.14) with $\beta > 1$ is extremely difficult to solve, even numerically. However, a reasonable estimate for \bar{z} can be obtained by approximating $P(z) = P(z - \bar{z})^0$ in the right-hand side of (6.17a). The result is

$$\beta\bar{z} = \sinh^{-1}[\chi_0(\beta)\eta'/2\Gamma], \quad (6.20)$$

where

$$\frac{1}{\chi_0(\beta)} = \int_{-\infty}^{\infty} dz P(z)^0 \cosh\beta z \quad (6.21a)$$

$$= \pi e^{\beta/4} / 2\mathbf{K}'(k)\sqrt{k}, \quad (6.21b)$$

with k such that $\beta = \pi\mathbf{K}'(k)/\mathbf{K}(k)$, where \mathbf{K} and \mathbf{K}' are the complete elliptic integrals.

A more accurate expression for \bar{z} can be derived in the limit $(\chi_0\eta'/\Gamma)^2 \gg 1$, where²⁹

$$\bar{z}^2 \gg \int_{-\infty}^{\infty} dz (z - \bar{z})^2 P(z). \quad (6.22)$$

To within corrections of order $\exp(-2\beta\bar{z})$, the distribution $P(z)$ approximates

$$P(z) = F_{\infty}(z - \bar{z}), \quad (6.23)$$

where, from (6.14),

$$(\eta'/\Gamma)[dF_{\infty}(z)/dz] = e^{\beta z} \{ e^{\beta(z+1)} F_{\infty}(z+1) - e^{\beta z} F_{\infty}(z) \}, \quad (6.24a)$$

or

$$F_{\infty}(z) = \chi(\beta) \int_z^{z+1} dz_1 e^{\beta z_1} F_{\infty}(z_1), \quad (6.24b)$$

with $\chi(\beta) = (\Gamma/\eta')e^{\beta\bar{z}}$. The function $F_{\infty}(z)$ has a vanishing first (z) moment but otherwise satisfies the same boundary conditions as $P(z)$. Values of $F_{\infty}(z)$ computed by numerical iteration of Eq. (6.24b) are plotted for different choices of $\beta \geq 2$ in Fig. 4. The curves differ from those of $P(z)^0$ in Fig. 1, principally in a small asymmetry about $z = 0$.

For this limiting case the magnitude of the combination $2\beta\bar{z}$ relevant to Eq. (6.19) depends upon the eigen-

²⁹ The condition $\kappa_m^2 \ll \frac{1}{3}$ requires from (3.7) that $\bar{z} \ll l(1 + L_e I_0 / \Phi_0) / 2\pi$, which will not be a serious restriction if l is large.

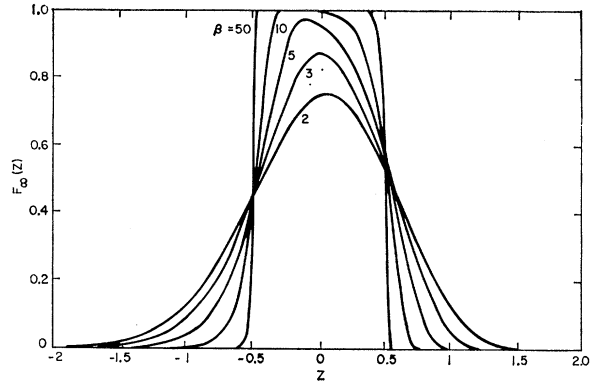


FIG. 4. Steady-state distribution function $F_{\infty}(z)$ of Eqs. (6.23) and (6.24) for different values of β .

value $\chi(\beta)$ of Eq. (2.14b).

$$|2\beta\bar{z}| = \ln(\eta'/\Gamma)^2 + \ln\chi^2(\beta), \quad (6.25)$$

where

$$\ln\chi^2(\beta) = -\beta + 2 \ln\beta - 2C_E + 2\beta \sum_{n=1}^{\infty} (e^{\beta n} - 1)^{-1}, \quad (6.26)$$

with $C_E = 0.57721566 \dots$ (Euler's constant). Equation (6.26) is derived in the Appendix along with an asymptotic expansion useful for $\beta \lesssim 2$.

In the limit $(\chi_0\eta'/\Gamma)^2 \gg 1$, Eq. (6.20) reduces to an expression of the form (6.25) but with $\chi_0(\beta)$ in place of $\chi(\beta)$. The difference $\ln\chi^2(\beta) - \ln\chi_0^2(\beta)$ is of order β^2 for β small and of order $\ln\beta$ for β large. These facts suggest that we can improve the estimate (6.20) by using $\chi(\beta)$

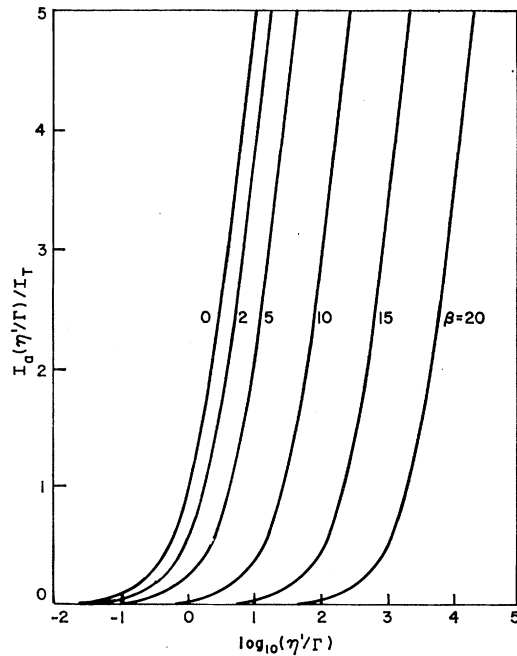


FIG. 5. Time-averaged steady-state current $I_a(\eta'/\Gamma)/I_T$ from Eq. (6.27) for different values of β .

in place of $\chi_0(\beta)$. The resulting expression is exact in the rapid-sweep-rate limit $(\chi\eta'/\Gamma)^2 \gg 1$ and is a convenient reasonably accurate interpolation for slower sweep rates. When used with Eq. (6.19), it gives

$$I_a(\eta')/I_T = 2 \sinh^{-1}[\chi(\beta)\eta'/2\Gamma]. \quad (6.27)$$

The ratio I_a/I_T is plotted as a function of (η'/Γ) for different values of β in Fig. 5.

The field sweep rate η' is slow in the sense required in Sec. VI A if $\bar{z} \ll 0.5$ or, equivalently, if

$$|\eta'| \ll [2\Gamma/\chi(\beta)] \sinh(\frac{1}{2}\beta). \quad (6.28)$$

For $\beta \lesssim 2$ this reduces to $|\eta'| \ll \Gamma\beta$; for $\beta \gg 1$ it reduces to $|\eta'| \ll \Gamma e^{\beta/2}$.

In the experiment of Lukens and Goodkind,¹⁰ the sweep rate η' is fixed, β has its saturation value β_∞ , and I_a is measured in units of $I_\Phi \equiv \Phi_0/L_s$ as a function of temperature below T_c . From the definitions (6.4) and (6.9b) and from Eqs. (6.19) and (6.27), it follows in this case that

$$I_a/I_\Phi = \bar{z} = \beta_\infty^{-1} \sinh^{-1}[\chi(\beta_\infty)\eta'/2\Gamma(T)]. \quad (6.29)$$

Temperature dependence enters through the transition rate $\Gamma(T)$.

VII. DISCUSSION

The results we have derived describe the effects of intrinsic fluctuations for T near but below T_c (bulk) in a closed superconducting ring having a thin weak-link section of uniform cross-sectional area $\sigma \ll \xi^2(T)$ and length $L \gg \xi(T)$. The intrinsic fluctuations are detectable only where they are not masked by extraneous fluctuations or noise. Extraneous temporal fluctuations can be eliminated by careful temperature control and by electromagnetic shielding.^{2,5,9,10} Spatial fluctuations (or inhomogeneities) in the superconductor, especially in the weak-link section, are much harder to control. The spatial scale is fixed by the coherence length $\xi(T)$; typically a micron or less. It is extraordinarily difficult to fabricate a homogeneous weak-link section on this scale. Webb and Warburton attempted to overcome this difficulty by using whisker crystals, wire-like crystals which grow remarkably free from defects and with good geometric uniformity.^{2,8} The range they measured of the resistive transition in simply connected samples was an order of magnitude smaller than that previously reported for thin films.⁶⁻⁸

Measurements on ring samples containing a whisker-crystal weak link have not yet been reported. The published data most directly relevant to our theory are those of Lukens and Goodkind on thin-film Sn rings.¹⁰ The agreement between theory and experiment is moderately good. Some of the discrepancies can be attributed to film homogeneities or to the fact that the thin-film weak links only marginally approximate a long thin wire. It is not yet clear whether all discrepancies are of this type or whether some reflect basic flaws in

TABLE I. Parameters for thin-film ring of Lukens and Goodkind.^a

A. Experiment ^{a-c}	
Cross section $\sigma = 3 \times 10^{-9}$ cm ²	
Length $L = 8 \times 10^{-4}$ cm	
Bulk/link dimensions $\sigma_b/\sigma = 330$, $l_b/l = 1870$	
$I_p(\text{sat})/I_\Phi = 0.32$	
$\log_{10}\Gamma(T) = 1.67(\Delta T_e - 10.3)$, $0.1 \lesssim \Gamma \lesssim 10$ sec ⁻¹	
$I_a(\Delta T)/I_\Phi = 0.319(\Delta T_e - 9.2)^{3/2}$, $ I_p \lesssim 5I_\Phi$, for $\eta' = 2$ sec ⁻¹	
B. Theory ^d	
$\beta_\infty = 4.5$	
Inductance $L_s = 9.3 \times 10^{-9}H$	
$\Delta T_\beta = 0.5 \pm 0.2$ m°K	
$I_0/\Delta T = (3.0 \pm 1.2) \times 10^{-6}$ A/m°K	
Mean free path (dirty limit) $= 200 \pm 100$ Å	
$l/(\Delta T)^{1/2} = 2.3 \pm 0.6(\text{m}^\circ\text{K})^{-1/2}$, $l = L/\xi(T)$	
$\Delta T = \Delta T_e - 1.0 \pm 0.3$ m°K	
$\Omega(T) = 10^{10}$ to 10^{12} sec ⁻¹	
$\Delta F(T)/k_B T_c (\Delta T)^{3/2} = 0.9 \pm 0.1$ (m°K) ^{-3/2}	

^a Reference 10.

^b Reference 28.

^c ΔT_e is measured from temperature where I_p extrapolates to zero.

^d Uncertainties reflect the fit of the theory to the data as given; no attempt was made to evaluate separately the intrinsic quality of the data.

the theory. Data on rings with whisker-crystal links would be useful.

Data of Lukens and Goodkind for the thin-film Sn rings described in Sec. I are summarized in Table I.^{10,28} The experimental temperature difference ΔT_e is measured from the temperature at which I_p extrapolates to zero [Fig. 3(b), Ref. 10] and is very near the low-temperature end of the resistive transition ($R < 0.01R_n$).²⁸ From the saturation value $I_p(\text{sat})/I_\Phi = 0.32$, we infer from Fig. 3(b) that $\beta_\infty = 4.5$ or $L_s = 9.3 \times 10^{-9}H$, which is reasonable for the geometry. Experimental values [Fig. 3(b), Ref. 10] of $I_p(\Delta T)/I_p(\text{sat})$ are plotted in Fig. 6 together with a theoretical curve derived from Eq. (6.9a) and Fig. 3(a). The choices $\Delta T = \Delta T_e - 1$ m°K and $\Delta T_\beta = 0.5$ m°K were used to optimize the fit. The difference $\Delta T - \Delta T_e = -1$ m°K derives from experimental uncertainty in $T_c(\text{bulk})$. The value of ΔT_β is consistent with Eqs. (3.2) and (6.9c) for Sn in the dirty limit with an electron mean free path of 200 Å, which is short but not unreasonable. Condition (5.10) is met for all $\Delta T \gg 0.5$ m°K; the theory is not expected to hold for $\Delta T \lesssim 0.5$ m°K.

These results, which test the static or equilibrium predictions of the theory, agree as well as one might reasonably expect for the experimental geometry. Lukens and Goodkind have also measured the rate $\Gamma(T)$. Their results can be expressed equally well (over the measurement interval $0.1 \lesssim \Gamma \lesssim 10$ sec⁻¹) by the expression in Table I or by either of the expressions

$$\Gamma(T) = \exp\{0.843[(9.3)^{3/2} - (\Delta T)^{3/2}]\} \text{sec}^{-1} \quad (7.1a)$$

or

$$\Gamma(T) = (\Delta T/9.3)^{9/4} \times \exp\{0.896[(9.3)^{3/2} - (\Delta T)^{3/2}]\} \text{sec}^{-1}, \quad (7.1b)$$

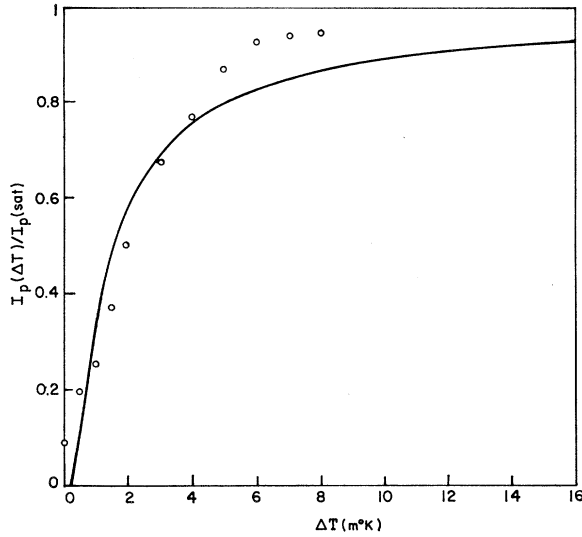


FIG. 6. Comparison of theory (solid line) and experiment (circles) for $I_p(\Delta T)/I_p(\text{sat})$ for a thin-film Sn ring as described by Lukens and Goodkind, Ref. 10. The experimental points are taken from Fig. 3(b), Ref. 10, with a temperature shift $\Delta T - \Delta T_e = -1$ m°K and with $I_p(\text{sat})/I_\Phi = 0.32$ as in Table I. The theoretical curve follows from Fig. 3(a) and Eq. (6.9a) with $\beta_\infty = 4.5$ and $\Delta T_\beta = 0.5$ m°K.

for ΔT in m°K. The first equation is appropriate to the form (5.5) of the prefactor $\Omega(T)$ in (6.11), the second to the form (5.8). With $\beta = \beta_\infty = 4.5$, those prefactors are, respectively,

$$\Omega(T) = e^{25.1} = 7.6 \times 10^{10} \text{ sec}^{-1} \quad (7.2a)$$

and

$$\Omega(T) = (\Delta T/9.3)^{9/4} \times e^{26.6} = 3.4(\Delta T/9.3)^{9/4} \times 10^{11} \text{ sec}^{-1}. \quad (7.2b)$$

The zero-current free-energy barrier $\Delta F(T) = l\Phi_0 I_0 \sqrt{2}/6\pi^2$ in the two cases (7.1) is, respectively,

$$\Delta F(T)/k_B T_e = 0.84(\Delta T)^{3/2} \quad (7.3a)$$

and

$$\Delta F(T)/k_B T_e = 0.90(\Delta T)^{3/2}, \quad (7.3b)$$

for ΔT in m°K. The expressions for l and I_0 deduced from the I_p data and listed in Table I give

$$\Delta F(T)/k_B T_e = 6.6(\Delta T)^{3/2}, \quad (7.4)$$

which is approximately one order of magnitude larger than both of the expressions (7.3).³⁰ We tentatively ascribe this discrepancy to inhomogeneities in the thin-film weak link.

Using Eq. (5.5) with $\tau = 10^{-12}$ sec and $n_e = 5 \times 10^{-22}$ cm⁻³, we estimate

$$\Omega(T) = 1.2 \times 10^{23} \text{ sec}^{-1}, \quad (7.5a)$$

³⁰ Because $\Delta F(T)$ appears in the exponent of (6.11), a factor-of-10 change in $\Delta F \gtrsim 20$ produces an enormous change in $\Gamma(T)$. Corresponding changes in the prefactor $\Omega(T)$ are much less important; they are easily absorbed by a small dilation of the ΔT temperature scale.

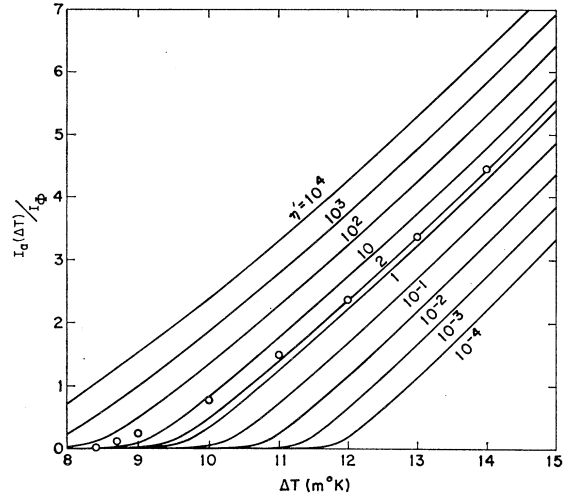


FIG. 7. Theoretical (solid lines) and experimental (circles) values of $I_a(\Delta T)/I_\Phi$ for the thin-film Sn ring described by Lukens and Goodkind, Ref. 10. For $|I_p| \leq 5I_\Phi$, the experimental points are adequately described (see Ref. 28) by $I_a(\Delta T)/I_\Phi = 0.319(\Delta T - 8.2)^{3/2}$, when $\eta' = 2 \text{ sec}^{-1}$. The theoretical curves follow from Eqs. (6.26) and (6.29) with $\beta_\infty = 4.5$ and $\Gamma(T)$ given by Eq. (7.1b).

which is twelve orders of magnitude greater than the experimental number (7.2a). Using the expressions for l and $\Delta F(T)$ as determined above and listed in Table I, we estimate from Eqs. (5.7) and (5.8) that

$$\Omega(T) = 1.7(\Delta T/9.3)^{9/4} \times 10^{10} \text{ sec}^{-1}, \quad (7.5b)$$

which is only a factor of 20 less than the experimental number (7.2b).³⁰ These results favor the prefactor (5.8) derived from the time-dependent Ginzburg-Landau theory, but other data^{2,28} favor the form (5.5) suggested by Langer and Ambegaokar. The issue remains unresolved.

Lukens and Goodkind also measured the average circulating current I_a as a function of temperature for $\eta(t) = \Phi_e(t)/\Phi_0$ increasing at a constant rate $\eta' = 2 \text{ sec}^{-1}$. [The oscillations of the ring current about I_a have a sinusoidal form (Fig. 3(a), Ref. 10) consistent with $\beta = 4.5$ in Fig. 2.] Their results^{10,28} are summarized in Table I and Fig. 7. The theoretical curves have been computed from Eqs. (6.26) and (6.29) with $\beta = 4.5$ as determined from $I_p(\text{sat})$ and with $\Gamma(T)$ given by the semiempirical Eq. (7.1b). No parameters were adjusted. The fit for $\eta' = 2$ is remarkably good, better than we have a right to expect considering the marginal geometry and probable inhomogeneities.

Further tests of the theory on systems with weak links which more nearly approximate the long one-dimensional uniform wire are required. Preferably each link should be tested with the superconducting ring intact and with it broken. In the latter case the Langer-Ambegaokar theory¹ should apply, perhaps with the modified prefactor (5.8).

The theory we have described is a statistical theory based upon the Ginzburg-Landau free energy. It is

only expected to accurately describe single-quantum transitions for T near but slightly below T_c [Eq. (5.10)]. Multiple-quantum transitions are not yet well understood nor is there a satisfactory theory of dissipation in one-dimensional weak links for $T \ll T_c$.

ACKNOWLEDGMENTS

I am grateful to B. I. Halperin and P. C. Hohenberg for insight into critical fluctuations, to J. K. Galt for comments on the manuscript and on other applications of the theory, to W. W. Webb for extensive discussions on whisker-crystal experiments, and especially to J. M. Goodkind and J. E. Lukens for patiently providing additional details of their thin-film measurements.

APPENDIX: EIGENVALUE $\chi(\beta)$ OF EQUATION (6.24b)

It is useful to introduce the two-sided Laplace transform $L(p)$ defined for all finite p by

$$L(p) = \int_{-\infty}^{\infty} dz F_{\infty}(z) e^{\beta pz}. \quad (\text{A1})$$

Taking the Laplace transform of Eq. (6.24a) and integrating the left-hand side by parts, we obtain

$$L(p)/L(p+1) = \chi(\beta) [(1 - e^{-\beta p})/\beta p], \quad (\text{A2})$$

where $\chi(\beta)$ is the eigenvalue to be determined. The normalization condition (6.16) implies

$$L(0) = 1, \quad (\text{A3})$$

which together with (A2) fixes $L(p)$ for all real integral p when $\chi(\beta)$ is known. The eigenvalue $\chi(\beta)$ is itself fixed by the condition implicit in (6.23) that

$$0 = \beta \int_{-\infty}^{\infty} dz z F_{\infty}(z) = \left(\frac{dL(p)}{dp} \right)_{p=0}. \quad (\text{A4})$$

The basic mathematical problem is to find the analytic function $L(p)$ which satisfies (A2) and (A3) for a given $\chi(\beta)$ and then to choose $\chi(\beta)$ such that (A4) is satisfied. We do this by two different methods. The first gives an asymptotic expansion for $\chi(\beta)$ useful for $\beta \lesssim 2$; the second gives the exact result (6.26).

If we define the function $N(p)$ such that

$$N(p) = \ln L(p), \quad (\text{A5})$$

it follows from (A2) that

$$N(p) - N(p+1) = \ln \chi(\beta) + \ln [(1 - e^{-\beta p})/\beta p] \quad (\text{A6a})$$

$$= \ln \chi(\beta) - \frac{1}{2} \beta p + \sum_{k=1}^{\infty} \frac{(\beta p)^{2k} B_{2k}}{2k(2k)!}, \quad (\text{A6b})$$

where B_{2k} is a Bernoulli number.³¹ If we assume that $N(p)$ can be expressed as a series of Bernoulli polynomials $B_n(p)$

$$N(p) = \sum_{n=0}^{\infty} a_n B_n(p), \quad (\text{A7})$$

it follows from (A6b) and the familiar property [GR 9.623(2)]³¹

$$B_n(p+1) - B_n(p) = n p^{n-1} \quad (\text{A8})$$

that

$$\begin{aligned} a_1 &= -\ln \chi(\beta), & a_{2k+1} &= -\beta^{2k} B_{2k}/2k(2k+1)(2k)!, \\ a_2 &= \frac{1}{4}\beta, & a_{2k+2} &= 0, \end{aligned} \quad (\text{A9})$$

for $k \geq 1$. With (A3), the condition (A4) is equivalent to [GR 9.623(3), GR 9.628(1)]

$$0 = \frac{dN(0)}{dp} = \sum_{n=0}^{\infty} a_n n B_{n-1}, \quad (\text{A10})$$

which with (A8) gives the asymptotically convergent series

$$\ln \chi^2(\beta) = \beta B_1 - \sum_{k=1}^{\infty} \beta^{2k} B_{2k}^2 / k(2k)! \quad (\text{A11a})$$

$$\begin{aligned} &= -\left(\frac{1}{2}\beta\right) - \frac{\left(\frac{1}{2}\beta\right)^2}{18} - \frac{\left(\frac{1}{2}\beta\right)^4}{2700} \\ &\quad - \frac{\left(\frac{1}{2}\beta\right)^6}{59\,535} - \frac{\left(\frac{1}{2}\beta\right)^8}{56\,7000} - \dots \end{aligned} \quad (\text{A11b})$$

This is useful for $\beta \lesssim 2$ but not for larger values.

To obtain the expression (6.26), we attack (A2) more directly. We recognize that the gamma function $\Gamma(z)$ has the property $\Gamma(z+1)/\Gamma(z) = z$ and exploit this fact in our solution. We rewrite (A2) in the form [GR 1.43(2)]

$$\begin{aligned} \frac{L(p)}{L(p+1)} &= \chi e^{-\frac{1}{2}\beta p} \frac{\sinh(\frac{1}{2}\beta p)}{\frac{1}{2}\beta p} \\ &= \chi e^{-\beta p/2} \prod_{n=1}^{\infty} \left(1 + \frac{p^2}{(2\pi n/\beta)^2} \right), \end{aligned} \quad (\text{A12})$$

and look for solutions of the form

$$L(p) = \frac{L_0 e^{\beta p(p-1)/4}}{\chi^p} \prod_{n=1}^{\infty} L_n(p), \quad (\text{A13})$$

where L_0 is a constant fixed by (A3), and where

$$L_n(p)/L_n(p+1) = 1 + p^2/(2\pi n/\beta)^2. \quad (\text{A14})$$

An acceptable solution of (A14) is

$$L_n(p) = (2\pi n/\beta)^{2p} / \Gamma(p + i2\pi n\rho\beta) \Gamma(p - i2\pi n\rho\beta). \quad (\text{A15})$$

³¹ Our notation corresponds closely to that in I. S. Gradshteyn and I. M. Ryzhik, *Table of Integrals, Series and Products* (Academic Press Inc., New York, 1965). Pertinent formulas from this reference are cited in the appendix text as, for example, GR 9.623(2).

Using this with (A5) and (A13), we have

$$N(p) = \ln L_0 + \frac{1}{4}\beta p(p-1) - p \ln \chi$$

$$+ \sum_{n=1}^{\infty} [p \ln(2\pi n/\beta)^2 - \ln \Gamma(p+i2\pi n/\beta) - \ln \Gamma(p-i2\pi n/\beta)] \quad (A16)$$

and

$$\frac{dN}{dp} = \frac{1}{2}\beta(p-\frac{1}{2}) - \ln \chi + \sum_{n=1}^{\infty} [\ln(2\pi n/\beta)^2 - \psi(p+i2\pi n/\beta) - \psi(p-i2\pi n/\beta)], \quad (A17)$$

where $\psi(z) = d \ln \Gamma(z) / dz$. We require [(A10)] that dN/dp vanish in the limit $p \rightarrow 0^+$ (positive real). We use the integral representation [GR 8.361(8)]

$$\psi(z) = \ln z + \int_{-0}^{\infty} dt e^{-tz} \left(\frac{1}{t} - \frac{1}{1-e^{-t}} \right) \quad (A18)$$

valid for $\text{Re} z > 0$ to obtain from (A17)

$$\ln \chi(\beta) = -\frac{1}{4}\beta + \lim_{p \rightarrow 0^+} \sum_{n=1}^{\infty} \left[\ln(2\pi n/\beta)^2 - \ln[p^2 + (2\pi n/\beta)^2] - 2 \int_0^{\infty} dt e^{-tp} \times \left(\frac{1}{t} - \frac{1}{1-e^{-t}} \right) \cos(2\pi nt/\beta) \right] \quad (A19a)$$

$$= -\frac{1}{4}\beta + \lim_{p \rightarrow 0^+} \int_0^{\infty} dt \left(\frac{1}{t} - \frac{e^{-tp}}{1-e^{-t}} \right) \times (\beta \sum_{n=0}^{\infty} \delta(t-n\beta) - 1), \quad (A19b)$$

where, because the lower limit of the integral is at $t=0$, the integrated area under the δ function at $t=0$ is only $\frac{1}{2}$. Relevant integrals for (A19b) are ($p=0^+$)

$$\beta \int_0^{\infty} dt \left(\frac{1}{t} - \frac{1}{1-e^{-t}} \right) \delta(t) = -\frac{1}{4}\beta; \quad (A20a)$$

$$\int_0^{\beta/2} dt \left(\frac{1}{t} - \frac{1}{1-e^{-t}} \right) = \ln(\frac{1}{2}\beta) - \ln(e^{\beta/2}-1); \quad (A20b)$$

$$\int_{\beta/2}^{\infty} dt \frac{1}{t} [\beta \sum_n \delta(t-n\beta) - 1] = \lim_{N \rightarrow \infty} \left(\sum_{n=0}^N n^{-1} - \ln(2N+1) \right) = C_E - \ln 2; \quad (A20c)$$

$$\int_{\beta/2}^{\infty} dt \frac{e^{-pt}}{1-e^{-t}} [\beta \sum_n \delta(t-n\beta) - 1] = \int_{\beta/2}^{\infty} dt \frac{e^{-t}}{1-e^{-t}} [\beta \sum_n \delta(t-n\beta) - 1] = \beta \sum_{n=1}^{\infty} (e^{n\beta}-1)^{-1} + \ln(1-e^{-\beta/2}). \quad (A20d)$$

Euler's constant C_E is defined in GR 8.367(2). Using these pieces in (A19b), we obtain

$$\ln \chi(\beta) = -\frac{1}{2}\beta + \ln \beta - C_E + \beta \sum_{n=1}^{\infty} (e^{\beta n} - 1)^{-1}, \quad (A21)$$

from which (6.26) follows immediately.